



Microwave dielectric properties of the $(1-x)\text{La}(\text{Nb}_{0.9}\text{V}_{0.1})\text{O}_4-x\text{CaMoO}_4$ ($0.05 \leq x \leq 0.50$) scheelite solid solution ceramics



Zhili Ma ^a, Jinxiong Zhao ^b, Di Zhou ^{c,*}

^a State Grid Gansu Electric Power Company, Lanzhou 730030, China

^b State Grid Gansu Electric Power Research Institute, Lanzhou 730070, China

^c Electronic Materials Research Laboratory, Key Laboratory of the Ministry of Education & International Center for Dielectric Research, School of Electronic and Information Engineering, Xi'an Jiaotong University, Xi'an 710049, China

ARTICLE INFO

Article history:

Received 8 January 2019
Received in revised form
2 March 2019
Accepted 4 March 2019
Available online 5 March 2019

Keywords:

Microwave dielectric
LaNbO₄
Low temperature co-fired ceramic (LTCC)

ABSTRACT

The CaMoO₄ was added into La(Nb_{0.9}V_{0.1})O₄ ceramics by solid state reaction method to adjust the temperature coefficient of frequency (TCF) values. The series of $(1-x)\text{La}(\text{Nb}_{0.9}\text{V}_{0.1})\text{O}_4-x\text{CaMoO}_4$ ($0.05 \leq x \leq 0.5$) ceramics were sintered at 1060–1180 °C and found to possess permittivity (ϵ_r) = 10.38–17.73, $Q \times f$ = 31,820–76,570 GHz ($Q = 1/\text{dielectric loss}$, f = resonant frequency lying between 8.5 and 9 GHz), and $\text{TCF} = -26.3 \sim +160.7$ ppm/°C. The structures of ceramic samples changed from monoclinic fergusonite to tetragonal scheelite continuously at $x = 0.20$ along with the shift of TCF values from positive to negative. The best microwave dielectric properties with $\epsilon_r = 15.71$, $Q \times f = 76,310$ GHz (at 8.825 GHz), and $\text{TCF} = -26.3$ ppm/°C were obtained in $0.8\text{La}(\text{Nb}_{0.9}\text{V}_{0.1})\text{O}_4-0.2\text{CaMoO}_4$ ceramics sintered at 1160 °C and these ceramics might be good candidates for microwave devices.

© 2019 Elsevier B.V. All rights reserved.

1. Introduction

Today, microwave dielectric ceramics are being studied by more and more people because of their universal application as dielectric resonators, filters, RF substrates and waveguides [1–3]. Generally, ceramics are prepared by conventional solid state reaction methods. The key point of this approach is mainly the presence of ceramic processing, which makes the ceramic compact enough. Microwave dielectric ceramics have been studied for decades to pursue good microwave dielectric properties, namely high $Q \times f$ ($Q = 1/\text{dielectric loss}$ and f = resonant frequency), high relative dielectric constant (ϵ_r) and near-zero resonant frequency temperature coefficient (TCF) [4–6]. Compared with the traditional perovskite (ABO₃) materials, recently the universal ABO₄ systems, including wolframite (MgWO₄), scheelite (CaWO₄), fergusonite (LaNbO₄), rutile (TiO₂) and zircon (NdVO₄) materials, have attracted more and more attention due to the structure adaptability [7–9].

It has been reported that the LaNbO₄ material transitions from fergusonite structure to scheelite structure at about 600 °C [10] and at the same time there is remarkable thermal expansion transition. Besides, there is a wide temperature gap 450–750 °C, which can be

revealed from Neutron and X-ray diffraction due to the existence of multicrystals [11,12]. Stubican et al. [13] noticed that the related phase transition temperature increased with decrease of rare earth ionic radius, and the niobates have lower phase transition temperatures than the corresponding tantalates. Based on the literatures' results, some researchers have provided solutions that use Ta instead of Nb or reduce the ionic radius of rare earth ions [14,15]. In 1980s, Bastide et al. [16] concluded that phase transition of ABX₄ ceramics according to the radius ratio of cation and anion. Subsequently, this work was supplemented by Manjon et al. [17], which mainly aimed at current research focusing on materials including orthorhombic, wolframite, fergusonite scheelite and zircon structures. It is well known that the phase evolution from high-temperature scheelite to low-temperature multicrystal is attributed to decrease of B-site cation [16–18]. Brik et al. [18] noticed that the phase transition temperature of LaNbO₄ ceramics could be adjusted to near room temperature in the manner of replacing by vanadium with smaller radius than niobium. Therefore, Brandão et al. [19] studied the influence of electrons and protons by scheelite retention.

Brower and Choi et al. reported microwave dielectric properties of the CaMoO₄ ceramics sintered at 1100 °C with $\epsilon_r = 10.8$ –11.7, $Q \times f = 55,000$ –89,700 GHz and $\tau_f = -50 \sim -60$ ppm/°C [20–24]. Vidya et al. [23] found that the CaMoO₄ nano-ceramics could be

* Corresponding author.

E-mail address: zhoudi1220@gmail.com (D. Zhou).

densified at a quite low sintering temperature $\sim 775^\circ\text{C}$. However, the large negative TCF of CaMoO_4 ceramic still limited the practical applications. Recently, a temperature stable LTCC (low temperature co-fired ceramics technology) materials have been achieved by using TiO_2 to adjust performance of the CaMoO_4 ceramics [23]. Meanwhile, Ca^{2+} in CaMoO_4 ceramics could be substituted for by $(\text{Li}_{0.5}\text{Bi}_{0.5})^{2+}$ ions and this resulted in near-zero TCF values [24]. Meanwhile, the low sintering temperatures of the $(\text{Li}_{0.5}\text{Bi}_{0.5})\text{MoO}_4$ – CaMoO_4 solid solution ceramics make them good candidates for LTCC technology [24,25]. We recently reported that the $\text{La}(\text{Nb}_{0.9}\text{V}_{0.1})\text{O}_4$ ceramics have good microwave dielectric properties including a large positive TCF value [26]. In the present study, we primarily researched the relation of microwave dielectric properties and structure of the $(1-x)\text{La}(\text{Nb}_{0.9}\text{V}_{0.1})\text{O}_4$ – $x\text{CaMoO}_4$ ceramics.

2. Experimental procedure

Reagent-grade raw materials of Nb_2O_5 (>99.5%, Guo-Yao Co. Ltd.), La_2O_3 (>99.95%, Guo-Yao Co. Ltd.), V_2O_5 (>99%, Fuchen Chemical Reagent, Tianjin, China), CaCO_3 (>99%, Guo-Yao Co. Ltd.) and MoO_3 (>99%, Guo-Yao Co. Ltd.) were measured according to the stoichiometric compositions of the $(1-x)\text{La}(\text{Nb}_{0.9}\text{V}_{0.1})\text{O}_4$ – $x\text{CaMoO}_4$ ($0.05 \leq x \leq 0.50$). La_2O_3 powders were treated at 1000°C for 5 h before weighting to remove carbonates. Powder mixtures were milled for 5 h using a planetary mill (QM-1F; Nanjing Machine Factory, Nanjing, China) at 200 rpm with the milling media (zirconia balls). After drying the mixtures were calcined at 800°C for 5 h and then re-milled at 250 rpm for 5 h to obtain fine powders. The fine powders were pressed into pellets (11 mm in diameter and 4–5 mm in height) with 5 wt % polyvinyl alcohol (PVA). All the samples were sintered in the air at 1000°C – 1200°C for 2 h.

Phase compositions and crystal structures of the $(1-x)\text{La}(\text{Nb}_{0.9}\text{V}_{0.1})\text{O}_4$ – $x\text{CaMoO}_4$ ($0.05 \leq x \leq 0.50$) ceramics were investigated using X-ray diffraction (XRD) with $\text{Cu K}\alpha$ radiation (Rigaku D/MAX-2400 X-ray diffractometer, Tokyo, Japan) and Rietveld refinement method was used to analyze the details of crystal structures. Microstructures were studied using a scanning electron microscopy (SEM; Quanta 250 F, FEI). Microwave dielectric properties were measured using the shielded resonant cavity method using the TE_{018} mode to calculate the permittivity and Q values, a network analyzer (8720 ES, Agilent, Palo Alto, CA), and a temperature chamber (Delta 9023, Delta Design, Poway, CA). The TCF/ τ_f values were obtained from the following formula:

$$\text{TCF} = \frac{f_T - f_{T_0}}{f_{T_0} \times (T - T_0)} \times 10^6 (\text{ppm}/^\circ\text{C}) \quad (1)$$

where f_T and f_{T_0} are the resonant frequencies at 85°C and 25°C , respectively.

3. Results and discussions

Fig. 1 shows XRD patterns of the $(1-x)\text{La}(\text{Nb}_{0.9}\text{V}_{0.1})\text{O}_4$ – $x\text{CaMoO}_4$ ($0 \leq x \leq 1$) ceramics sintered at their optimal temperatures for 2 h, which can help us understand the mechanism of two kinds of phase transition. The lattice parameters of pure $\text{La}(\text{Nb}_{0.9}\text{V}_{0.1})\text{O}_4$ ceramic were calculated to be $a = 5.508(9)$ Å, $b = 11.603(8)$ Å, $c = 5.236(0)$ Å, $\beta = 94.920^\circ$, and cell volume = $334.274(4)$ Å³. As the substitution content increased, the phase transition from fergusonite to tetragonal scheelite structure can be clearly observed from XRD patterns. In the range $0 \leq x \leq 0.1$, the $(1-x)\text{La}(\text{Nb}_{0.9}\text{V}_{0.1})\text{O}_4$ – $x\text{CaMoO}_4$ ceramics belong to a fergusonite solid solution with a space group $I2/a$. It was clearly seen from Fig. 1, XRD reflection peaks (-121) and (121) of $(1-x)\text{La}(\text{Nb}_{0.9}\text{V}_{0.1})\text{O}_4$ – $x\text{CaMoO}_4$

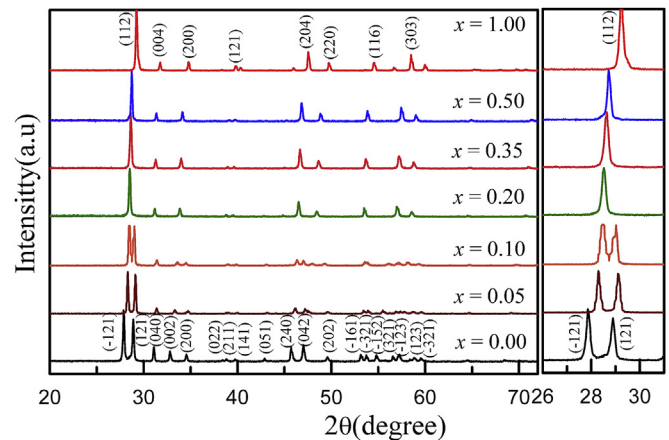


Fig. 1. XRD patterns of the $(1-x)\text{La}(\text{Nb}_{0.9}\text{V}_{0.1})\text{O}_4$ – $x\text{CaMoO}_4$ ($0 \leq x \leq 1$) ceramics sintered at their optimal temperatures.

($0 \leq x \leq 0.1$) ceramics moved to each other continuously with increase in CaMoO_4 contents. Finally at $x = 0.2$, (-121) and (121) merged into one peak (112) , which indicates that crystal structure of the $(1-x)\text{La}(\text{Nb}_{0.9}\text{V}_{0.1})\text{O}_4$ – $x\text{CaMoO}_4$ ceramics changed from fergusonite to scheelite. Fig. 2 shows the variations in lattice parameters of the $(1-x)\text{La}(\text{Nb}_{0.9}\text{V}_{0.1})\text{O}_4$ – $x\text{CaMoO}_4$ ceramics. As CaMoO_4 content increased, lattice parameters a , b and β ($\beta > 90^\circ$) in the solid solution region ($x \leq 0.1$) decreased slowly. Lattice parameters c increased slightly. With further increase of x value, the a and c values became equal to each other. Meanwhile, the b increased to $11.430(3)$ Å at $x = 0.2$ in tetragonal structure. The variation of lattice parameters clearly suggested the phase transition from fergusonite to scheelite structure in the $(1-x)\text{La}(\text{Nb}_{0.9}\text{V}_{0.1})\text{O}_4$ – $x\text{CaMoO}_4$ ceramics. These changes are in accordance with XRD results analysis. In order to research the details of crystal structure, Rietveld refinements were performed to study the crystal structure of the $0.9\text{La}(\text{Nb}_{0.9}\text{V}_{0.1})\text{O}_4$ – 0.1CaMoO_4 and $0.8\text{La}(\text{Nb}_{0.9}\text{V}_{0.1})\text{O}_4$ – 0.2CaMoO_4 ceramics. The Rietveld refinement results are presented in Fig. 3. The space group, occupancies and atomic positions are given in the Table 1 ($R_p = 9.94\%$, $R_{wp} = 12.9\%$, and $R_{exp} = 7.06\%$) and all the refinement results are acceptable. The $0.9\text{La}(\text{Nb}_{0.9}\text{V}_{0.1})\text{O}_4$ – 0.1CaMoO_4 ceramic belongs to single fergusonite phase with a space group $I2/a$. The $0.8\text{La}(\text{Nb}_{0.9}\text{V}_{0.1})\text{O}_4$ – 0.2CaMoO_4 ceramic belongs to standard scheelite structure with a space group $I4_1/a$

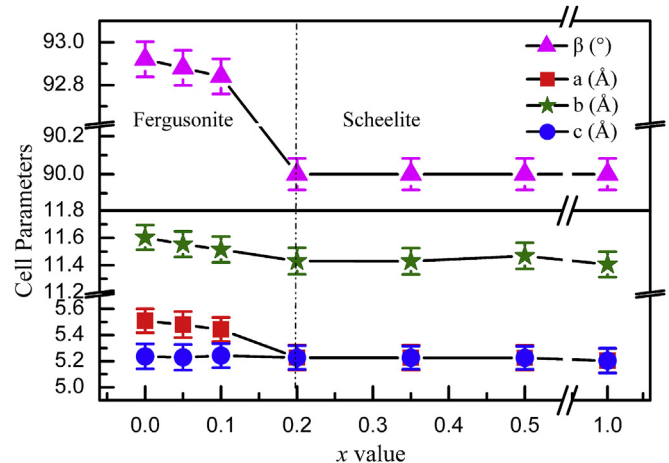


Fig. 2. Lattice parameters variation in the $(1-x)\text{La}(\text{Nb}_{0.9}\text{V}_{0.1})\text{O}_4$ – $x\text{CaMoO}_4$ ($0 \leq x \leq 1$) ceramics.

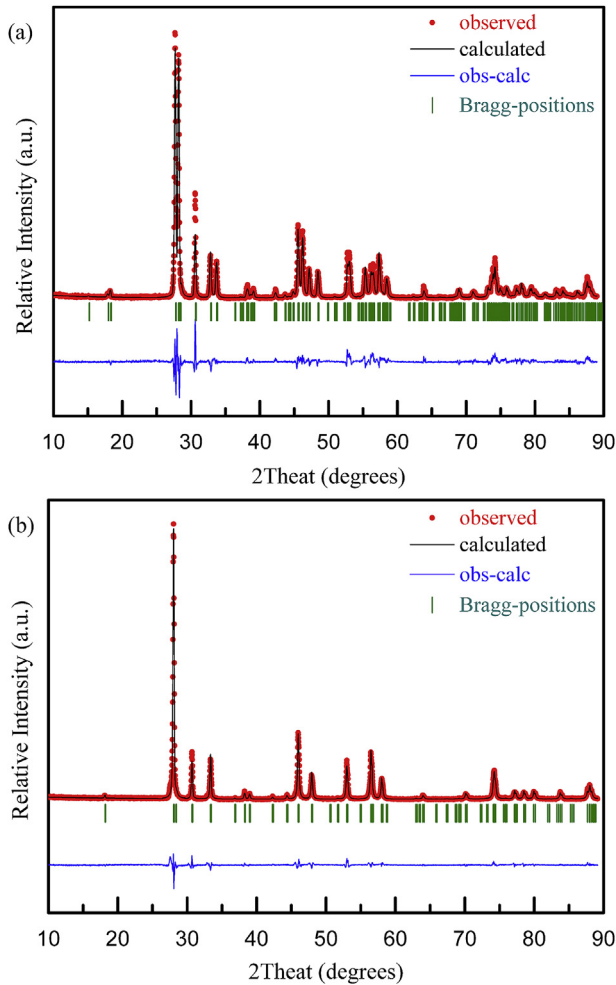


Fig. 3. Observed XRD (red points) and calculated pattern (black solid line) along with difference plot (at the bottom) of (a) the $0.9\text{La}(\text{Nb}_{0.9}\text{V}_{0.1})\text{O}_4\text{-}0.1\text{CaMoO}_4$ ceramics and (b) the $0.8\text{La}(\text{Nb}_{0.9}\text{V}_{0.1})\text{O}_4\text{-}0.2\text{CaMoO}_4$ ceramics. Allowed Bragg reflections are indicated by vertical bars and goodness-of-fit shown in inset. (For interpretation of the references to colour in this figure legend, the reader is referred to the Web version of this article.)

accordingly.

SEM results of the $(1-x)\text{La}(\text{Nb}_{0.9}\text{V}_{0.1})\text{O}_4\text{-}x\text{CaMoO}_4$ ceramics sintered at 1160°C are shown in Fig. 4. The dense micro-structure of the $(1-x)\text{La}(\text{Nb}_{0.9}\text{V}_{0.1})\text{O}_4\text{-}x\text{CaMoO}_4$ ceramics can be observed with almost no pores. With the increase of CaMoO_4 contents, grains of the ceramics become more homogeneous and very uniform grain distribution can be observed in the $0.8\text{La}(\text{Nb}_{0.9}\text{V}_{0.1})\text{O}_4\text{-}0.2\text{CaMoO}_4$ ceramic. Fig. 5 shows the variation of densities of the $(1-x)\text{La}(\text{Nb}_{0.9}\text{V}_{0.1})\text{O}_4\text{-}x\text{CaMoO}_4$ ($0.05 \leq x \leq 0.5$) ceramics as a function of sintering temperature. All the $(1-x)\text{La}(\text{Nb}_{0.9}\text{V}_{0.1})\text{O}_4\text{-}x\text{CaMoO}_4$ ceramics can be well densified in wide sintering temperatures. Due to the atomic weight differences, the increase of CaMoO_4 content apparently resulted in decrease of the bulk densities.

Variation of permittivity and $Q \times f$ values of the $(1-x)\text{La}(\text{Nb}_{0.9}\text{V}_{0.1})\text{O}_4\text{-}x\text{CaMoO}_4$ ($0.05 \leq x \leq 0.50$) ceramics as a function of sintering temperature are shown in Fig. 6. All the permittivity values keep stable in a quite wide sintering temperature range as shown in Fig. 6(a) and this is in accordance with the change trend of bulk density. The largest permittivity about 17.63 was obtained in the $0.95\text{La}(\text{Nb}_{0.9}\text{V}_{0.1})\text{O}_4\text{-}0.05\text{CaMoO}_4$ ceramic. Variation of $Q \times f$ values of the $(1-x)\text{La}(\text{Nb}_{0.9}\text{V}_{0.1})\text{O}_4\text{-}x\text{CaMoO}_4$ ($0.05 \leq x \leq 0.50$) ceramics as a function of sintering temperature are shown in Fig. 6(b) (resonant frequency lying between 8.5 and 9 GHz). $Q \times f$ values increase with sintering temperature first, and then decrease due to secondary grain growth at high temperatures. The $0.8\text{La}(\text{Nb}_{0.9}\text{V}_{0.1})\text{O}_4\text{-}0.2\text{CaMoO}_4$ ceramics sintered at 1160°C possess the highest $Q \times f$ values $\sim 76,310$ GHz at 8.825 GHz.

Fig. 7 shows microwave dielectric permittivity and $Q \times f$ values of the $(1-x)\text{La}(\text{Nb}_{0.9}\text{V}_{0.1})\text{O}_4\text{-}x\text{CaMoO}_4$ ($0 \leq x \leq 1$) ceramics as a function of CaMoO_4 content. Generally, permittivity is determined by dielectric polarization. In range of microwave frequency, dielectric polarization is the sum of both ionic and electronic components [27]. Shannon et al. [27] suggested that molecular polarizability could be estimated as the sum of individual ionic polarizabilities. Hence, polarizabilities (α_x) of the $(1-x)\text{La}(\text{Nb}_{0.9}\text{V}_{0.1})\text{O}_4\text{-}x\text{CaMoO}_4$ ceramics could be obtained as follows:

$$\alpha_x = (1-x)\alpha_{\text{La}^{3+}} + 0.9(1-x)\alpha_{\text{Nb}^{5+}} + 0.1(1-x)\alpha_{\text{V}^{5+}} + x\alpha_{\text{Ca}^{2+}} + x\alpha_{\text{Mo}^{6+}} + 4\alpha_{\text{O}^{2-}} \quad (2)$$

where $\alpha_{\text{La}^{3+}}$, $\alpha_{\text{Nb}^{5+}}$, $\alpha_{\text{V}^{5+}}$, $\alpha_{\text{Ca}^{2+}}$, $\alpha_{\text{Mo}^{6+}}$ and $\alpha_{\text{O}^{2-}}$ are polarizabilities of La^{3+} , Nb^{5+} , V^{5+} , Ca^{2+} , Mo^{6+} and O^{2-} ions [27]. Using the Clausius-Mosotti relation, the dielectric permittivity can be calculated as follows:

Table 1

Crystallographic parameters of the $0.9\text{La}(\text{Nb}_{0.9}\text{V}_{0.1})\text{O}_4\text{-}0.1\text{CaMoO}_4$ and the $0.8\text{La}(\text{Nb}_{0.9}\text{V}_{0.1})\text{O}_4\text{-}0.2\text{CaMoO}_4$ ceramics ($R_p = 9.94\%$, $R_{wp} = 12.9\%$, and $R_{exp} = 7.06\%$).

x	Atom	x	y	z	Occupancy	Mult
Space group: $I2/a$						
0.1	Ca	0.25000	0.12327	0.00000	0.050	4
	La1	0.25000	0.12327	0.00000	0.450	4
	Nb1	0.25000	0.63214	0.00000	0.405	4
	V1	0.25000	0.63214	0.00000	0.045	4
	Mo1	0.25000	0.63214	0.00000	0.050	4
	O1	0.01472	0.71352	0.16672	1.000	8
	O2	0.91465	0.45835	0.24286	1.000	8
Space group: $I4_1/a$						
0.2	Ca	0.00000	0.25000	0.62500	0.050	4
	La1	0.00000	0.25000	0.62500	0.200	4
	Nb1	0.00000	0.25000	0.12500	0.180	4
	V1	0.00000	0.25000	0.12500	0.020	4
	Mo1	0.00000	0.25000	0.12500	0.050	4
	O1	0.15684	0.00500	0.20917	1.000	16

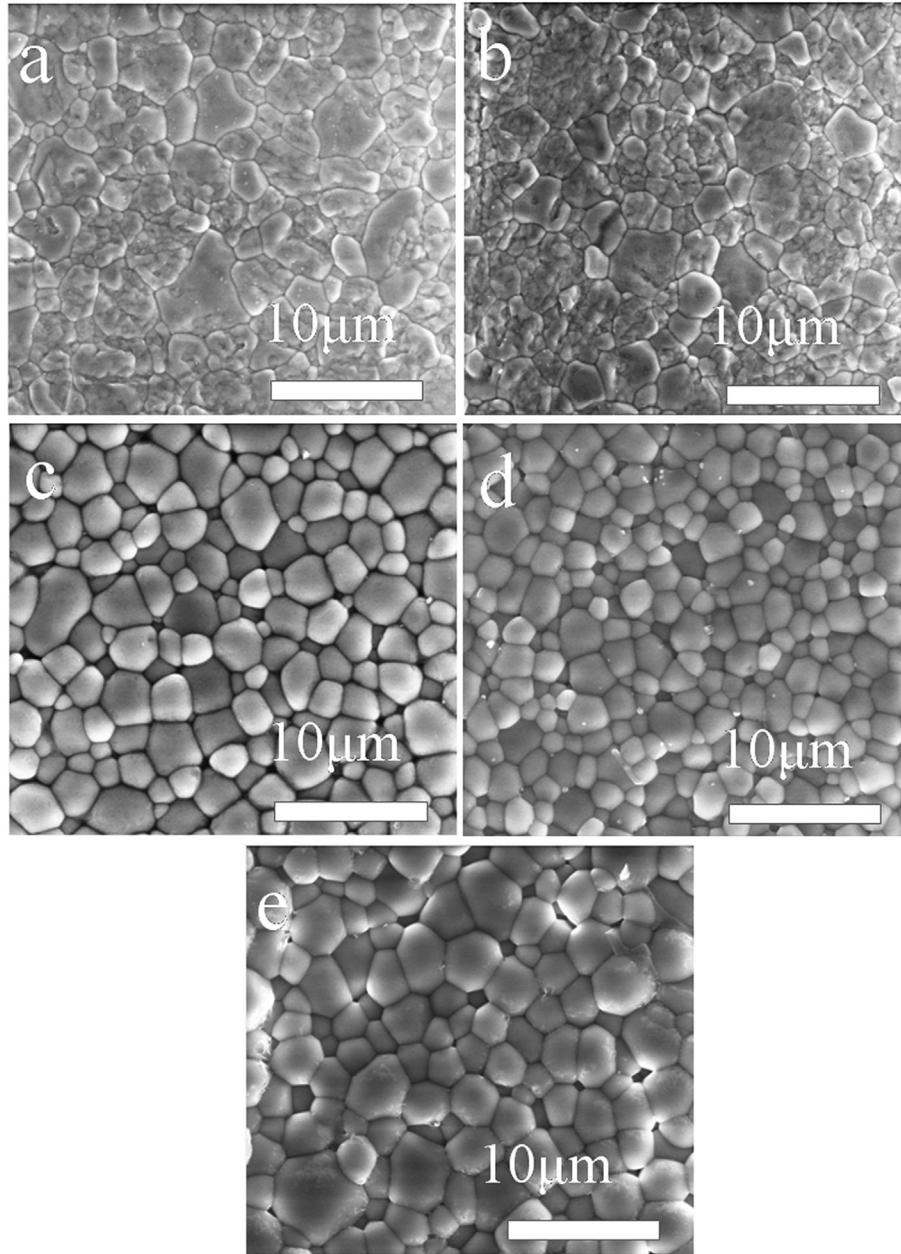


Fig. 4. SEM images of the $(1-x)\text{La}(\text{Nb}_{0.9}\text{V}_{0.1})\text{O}_4-x\text{CaMoO}_4$ (a) $x = 0.05$, (b) $x = 0.10$, (c) $x = 0.20$, (d) $x = 0.35$, (e) $x = 0.50$ ceramics sintered at 1160°C for 2 h.

$$\varepsilon_x = \frac{3V_x + 8\pi\alpha_x}{3V_x - 4\pi\alpha_x} \quad (3)$$

in which V_x is the cell volume ($= 336.695/4 = 84.17 \text{ \AA}^3$). Fig. 7(a) shows that ε_{cal} and ε_r of the $(1-x)\text{La}(\text{Nb}_{0.9}\text{V}_{0.1})\text{O}_4-x\text{CaMoO}_4$ ceramics gradually decrease as the increase of CaMoO_4 content due to the smaller ionic polarizability of Ca^{2+} and Mo^{6+} than that of La^{3+} and Nb^{5+} . $Q \times f$ values of the CaMoO_4 and $\text{La}(\text{Nb}_{0.9}\text{V}_{0.1})\text{O}_4$ ceramics are about 90,000 GHz and 60,000 GHz, respectively, as reported in literatures [21,26]. As shown in Fig. 7(b), $Q \times f$ values increase with the content of CaMoO_4 as expected. Quite high $Q \times f$ values were obtained in the solid solution ceramics due to the good sinterability that resulted in homogeneous microstructures. The $0.8\text{La}(\text{Nb}_{0.9}\text{V}_{0.1})\text{O}_4-0.2\text{CaMoO}_4$ ceramic possesses the highest $Q \times f$ value about

76,310 GHz at 8.825 GHz. The TCF values as a function of x value are presented in Fig. 7(c). It can be seen that the TCF values are large positive within monoclinic fergusonite solid solution region ($x < 0.2$) and this is in accordance with results in the $\text{La}(\text{Nb},\text{V})\text{O}_4$ system [26]. Introduction of CaMoO_4 into the $\text{La}(\text{Nb}_{0.9}\text{V}_{0.1})\text{O}_4$ lowered the ferroelastic phase transition temperature to near room temperature, resulting in composition-sensitive and unstable TCF values. When $x \geq 0.2$, the TCF values keep negative and increase with the CaMoO_4 content in scheelite region, which is quite normal in solid solution ceramics. The smallest TCF value about $-26.3 \text{ ppm}/^\circ\text{C}$ was obtained in the $0.8\text{La}(\text{Nb}_{0.9}\text{V}_{0.1})\text{O}_4-0.2\text{CaMoO}_4$ ceramics. The intrinsic microwave dielectric properties were studied by far-infrared spectra as shown in Fig. S1 and Table S1. All the fitted and measured values were found to be in good agreements.

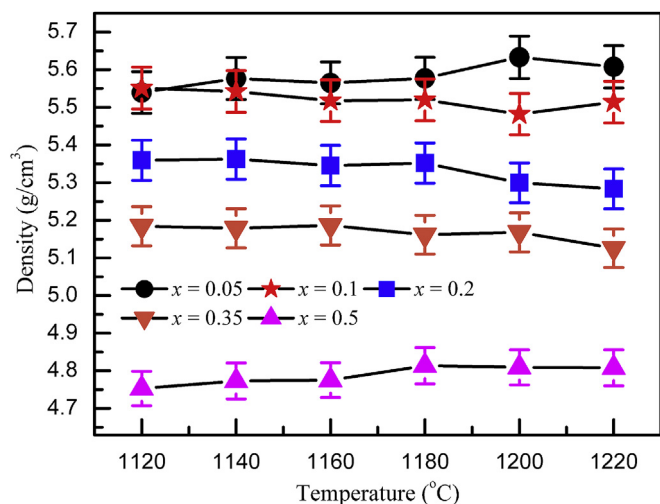


Fig. 5. Variation of density of the $(1-x)\text{La}(\text{Nb}_{0.9}\text{V}_{0.1})\text{O}_4-x\text{CaMoO}_4$ ($0.05 \leq x \leq 0.5$) ceramics as a function of sintering temperature.

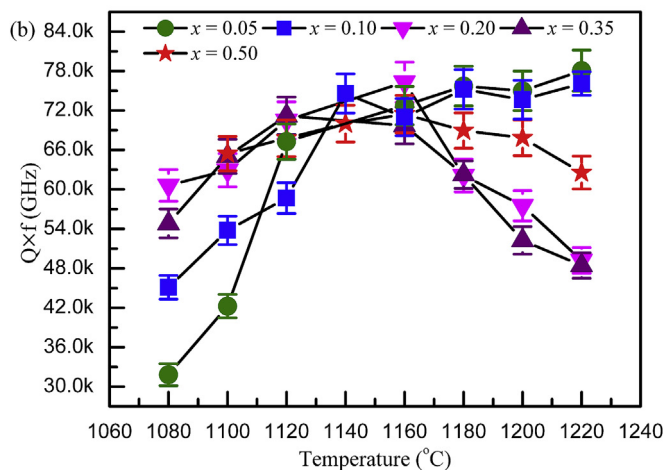
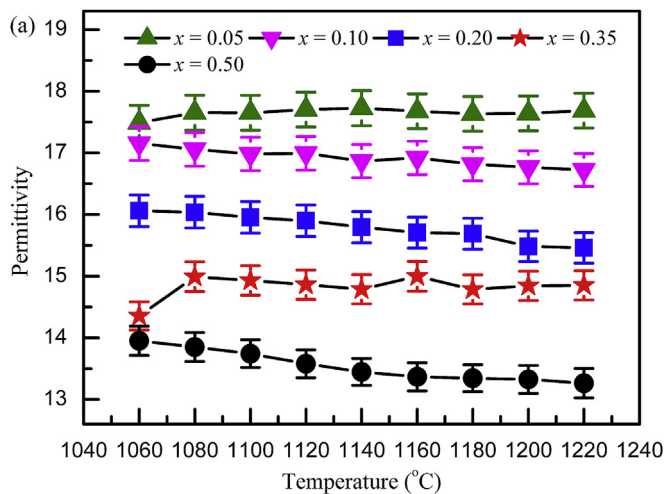


Fig. 6. Variation of permittivity (a) and $Q \times f$ values (b) of the $(1-x)\text{La}(\text{Nb}_{0.9}\text{V}_{0.1})\text{O}_4-x\text{CaMoO}_4$ ($0.05 \leq x \leq 0.50$) ceramics as a function of sintering temperature.

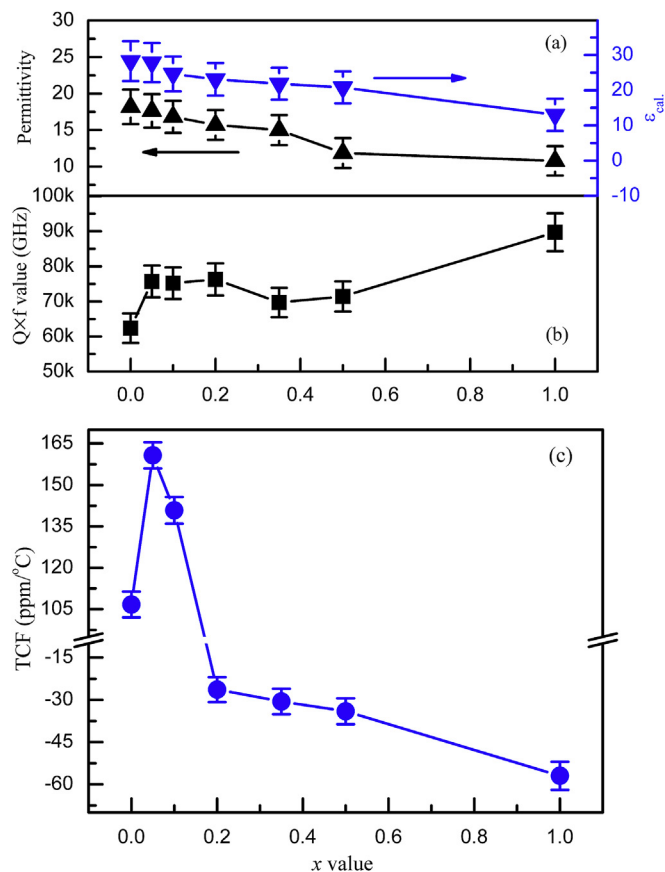


Fig. 7. ϵ_{ca1} and ϵ_r (a), $Q \times f$ value (b), and TCF (c) of the $(1-x)\text{La}(\text{Nb}_{0.9}\text{V}_{0.1})\text{O}_4-x\text{CaMoO}_4$ ($0 \leq x \leq 1$) ceramics as a function of x value.

4. Conclusions

The $0.65\text{La}(\text{Nb}_{0.9}\text{V}_{0.1})\text{O}_4-0.35\text{CaMoO}_4$ ceramic sintered at 1160°C was found to possess a $\epsilon_r = 15.00$, a $Q \times f = 69,720$ GHz at 9 GHz, and a $\text{TCF}/\tau_f = -30.6$ ppm/°C. The best microwave dielectric properties were obtained in the $0.8\text{La}(\text{Nb}_{0.9}\text{V}_{0.1})\text{O}_4-0.2\text{CaMoO}_4$ ceramics sintered at 1160°C with a $\epsilon_r = 15.71$, a $Q \times f = 76,310$ GHz at 8.825 GHz, and $\tau_f = -26.3$ ppm/°C. The XRD analysis reveals that the ceramics changed from monoclinic fergusonite to tetragonal sheelite phase at $x = 0.2$. Far-infrared reflectivity fitting of the $0.65\text{La}(\text{Nb}_{0.9}\text{V}_{0.1})\text{O}_4-0.35\text{CaMoO}_4$ ceramic shows that the main polarization comes from ionic polarization rather than electronic ones. These materials are very promising candidates for high quality microwave devices.

Acknowledgments

This work was supported by the State Grid Science and Technology Projects (China, 522722180007), the National Key Research and Development Program of China (2017YFB0406301), the National Natural Science Foundation of China (U1632146), the Key Basic Research Program of Shaanxi Province (2017GY-129), and the Fundamental Research Funds for the Central University. The authors would like to thank the administrators in IR beamline workstation (BL01B) of National Synchrotron Radiation Laboratory (NSRL) for their help in the IR measurement and fitting. The SEM work was done at the International Center for Dielectric Research (ICDR), Xi'an Jiaotong University, Xi'an, China and the authors thank Ms. Yan-Zhu Dai for her help in using SEM.

Appendix A. Supplementary data

Supplementary data to this article can be found online at <https://doi.org/10.1016/j.jallcom.2019.03.057>.

References

- [1] I.M. Reaney, D. Iddles, Microwave dielectric ceramics for resonators and filters in mobile phone networks, *J. Am. Ceram. Soc.* 89 (2006) 2063–2072.
- [2] D. Zhou, L.X. Pang, D.W. Wang, C. Li, B.B. Jin, I.M. Reaney, High permittivity, low loss microwave dielectrics suitable for 5G resonator and low temperature co-fired ceramic architecture, *J. Mater. Chem. C* 5 (2017) 10094–10098.
- [3] L.X. Pang, D. Zhou, Z.M. Qi, W.G. Liu, Z.X. Yue, I.M. Reaney, Structure-property relationships of low sintering temperature scheelite-structured $(1-x)\text{BiVO}_4-x\text{LaNbO}_4$ microwave dielectric ceramics, *J. Mater. Chem. C* 5 (2017) 2695–2701.
- [4] H. Hughes, D.M. Iddles, I.M. Reaney, Niobate-based microwave dielectrics suitable for third generation mobile phone base stations, *Appl. Phys. Lett.* 79 (2001) 2952–2954.
- [5] S.M. Moussa, J.B. Claridge, M.J. Rosseinsky, S. Clarke, $\text{Ba}_8\text{ZnTa}_6\text{O}_{24}$: a high-Q microwave dielectric from a potentially diverse homologous series, *Appl. Phys. Lett.* 82 (2003) 4537–4539.
- [6] A.G. Belous, O.V. Ovchar, M. Valant, D. Suvorov, Anomalies in the temperature dependence of the microwave dielectric properties of $\text{Ba}_{6-x}\text{Sm}_{8+2x/3}\text{Ti}_{18}\text{O}_{54}$, *Appl. Phys. Lett.* 77 (2000) 1707–1709.
- [7] V. Thangadurai, C. Knittlmayer, W. Weppner, Metathetic room temperature preparation and characterization of scheelite-type ABO_4 ($A = \text{Ca}, \text{Sr}, \text{Ba}, \text{Pb}; B = \text{Mo}, \text{W}$) powders, *Mater. Sci. Eng. B* 106 (2004) 228–233.
- [8] L.X. Pang, D. Zhou, Modification of NdNbO_4 microwave dielectric ceramic by Bi substitutions, *J. Am. Ceram. Soc.* (2019), <https://doi.org/10.1111/jace.16290>.
- [9] S.A. Tamura, New polymorphic transition of FeTaO_4 under high pressure, *Solid State Commun.* 12 (1973) 597–598.
- [10] T. Møkkelbost, H.L. Lein, P.E. Vullum, R. Holmestad, T. Grande, M. Einarsrud, Thermal and mechanical properties of LaNbO_4 -based ceramics, *Ceram. Int.* 35 (2009) 2877–2883.
- [11] L. Malavasi, C. Ritter, G. Chiodelli, Investigation of the high temperature structural behavior of $\text{La}_{0.99}\text{Ca}_{0.01}\text{NbO}_4$ proton conducting material, *J. Alloys Compd.* 475 (2009) L42–L45.
- [12] A.T. Aldred, M.V. Nevitt, S.K. Chan, The effect of surface constraint and finite particle-size on a continuous transformation. 2. experimental-observations on a vanadium-substituted lanthanum niobate, *J. Mater. Sci. Lett.* 4 (1985) 867–871.
- [13] V.S. Stubican, High-temperature transition in rare-earth niobates and tantalates, *J. Am. Ceram. Soc.* 47 (1964) 55–58.
- [14] R. Haugsrud, T. Norby, Proton conduction in rare-earth ortho-niobates and ortho-tantalates, *Nat. Mater.* 5 (2006) 193–196.
- [15] F. Vullum, F. Nitsche, S.M. Selbach, T. Grande, Solid solubility and phase transitions in the system $\text{LaNb}_{1-x}\text{Ta}_x\text{O}_4$, *Solid State Chem.* 181 (2008) 2580–2585.
- [16] J.P. Bastide, Simplified systematic of the compounds ABX_4 ($X = \text{O}^{2-}, \text{F}^-$) and possible evolution of their crystal-structures under pressure, *J. Solid Chem.* 71 (1987) 115–120.
- [17] F.J. Manjon, D. Errandonea, J. Lopez-Solano, P. Rodríguez-Hernández, S. Radescu, A. Mujica, A. Muñoz, N. Garro, J. Pellicer-Porres, A. Segura, Ch. Ferrer-Roca, R.S. Kumar, O. Tschauer, G. Aquilanti, Crystal stability and pressure-induced phase transitions in scheelite AWO_4 ($A = \text{Ca}, \text{Sr}, \text{Ba}, \text{Pb}, \text{Eu}$) binary oxides, *Phys. Stat. Sol. (b)* 244 (2007) 295–302.
- [18] F. Brik, R. Enjalbert, J. Galy, Synthesis, Crystal-growth and crystal structure of a scheelite type compound in lanthanum niobium vanadium oxygen system, *Mater. Res. Bull.* 29 (1994) 15–22.
- [19] A.D. Brandão, I. Antunes, J.R. Frade, J. Torre, V.V. Kharton, D.P. Fagg, Enhanced low-temperature proton conduction in $\text{Sr}_{0.02}\text{La}_{0.98}\text{NbO}_{4-\delta}$ by scheelite phase retention, *Chem. Mater.* 22 (2010) 6673–6683.
- [20] W.S. Brower, P.H. Fang, Dielectric constants of PbMoO_4 and CaMoO_4 , *Phys. Rev.* 149 (1966), 646–646.
- [21] G.K. Choi, J.R. Kim, S.H. Yoon, K.S. Hong, Microwave dielectric properties of scheelite ($A = \text{Ca}, \text{Sr}, \text{Ba}$) and wolframite ($A = \text{Mg}, \text{Zn}, \text{Mn}$) AMoO_4 compounds, *J. Eur. Ceram. Soc.* 27 (2007) 3063–3067.
- [22] S. Vidya, S. Solomon, J.K. Thomas, Synthesis, sintering and optical properties of CaMoO_4 : a promising scheelite LTCC and photoluminescent material, *Phys. Status Solidi A* 209 (2012) 1067–1074.
- [23] J. Guo, D. Zhou, L. Wang, H. Wang, T. Shao, Z.M. Qi, X. Yao, Infrared spectra, Raman spectra, microwave dielectric properties and simulation for effective permittivity of temperature stable ceramic $\text{AMoO}_4\text{-TiO}_2$ ($A = \text{Ca}, \text{Sr}$), *Dalton Trans.* 42 (2013) 1483–1491.
- [24] D. Zhou, H. Wang, Q.P. Wang, X.G. Wu, J. Guo, G.Q. Zhang, L. Shui, X. Yao, C.A. Randall, L.X. Pang, H.C. Liu, Microwave dielectric properties and Raman spectroscopy of scheelite solid solution $[(\text{Li}_{0.5}\text{Bi}_{0.5})_{1-x}\text{Ca}_x]\text{MoO}_4$ ceramics with ultra-low sintering temperatures, *Funct. Mater. Lett.* 3 (2010) 253–257.
- [25] D. Zhou, D. Guo, W.B. Li, L.X. Pang, X. Yao, D.W. Wang, I.M. Reaney, Novel temperature stable high- ϵ_r microwave dielectrics in the $\text{Bi}_2\text{O}_3\text{-TiO}_2\text{-V}_2\text{O}_5$ system, *J. Mater. Chem. C* 4 (2016) 5357–5362.
- [26] D. Guo, D. Zhou, W.B. Li, L.X. Pang, Y.Z. Dai, Z.M. Qi, Phase evolution, crystal structure, and microwave dielectric properties of water-insulation $(1-x)\text{LaNbO}_4\text{-LaVO}_4$ ($0 \leq x \leq 0.9$), *Inorg. Chem.* 56 (2017) 9321–9329.
- [27] R.D. Shannon, Dielectric polarizabilities of ions in oxides and fluorides, *J. Appl. Phys.* 73 (1993) 348–366.